Research Square

Preprints are preliminary reports that have not undergone peer review.
They should not be considered conclusive, used to inform clinical practice,
or referenced by the media as validated information.

Multi-Objective Ship Route Planning in Complex Ocean Environments Using an Environment-Aware Adaptive Ant Colony Optimization Algorithm

Qiang Yuan

yuanqiang@zjou.edu.cn

Zhejiang Ocean University

Yujie Jiang

Zhejiang Ocean University

Junsong Lei

Shanghai Marine Equipment Research Institute

Yu Yang

Zhejiang Ocean University

Baokui Wang

Zhejiang Ocean University

Jun Ye

Wuhan University of Technology

Fei Dong

Zhejiang Ocean University

Research Article

Keywords: Ship route planning, Ant colony optimization, Multi - objective optimization, Environmental awareness, Energy consumption model, ERA5, Ocean environment

Posted Date: August 25th, 2026

DOI: https://doi.org/10.21203/rs.3.rs-10048946/v1

License: This work is licensed under a Creative Commons Attribution 4.0 International License.
Read Full License

Additional Declarations: No competing interests reported.

Multi-Objective Ship Route Planning in Complex Ocean Environments Using an Environment-Aware Adaptive Ant Colony Optimization Algorithm

Qiang yuan 1*, Yujie Jiang 1, Junsong Lei 2, Yu Yang 1, Baokui Wang 1, Jun Ye 3, Fei Dong 1.

1 School of Naval Architecture and Maritime, Zhejiang Ocean University, Zhoushan 316022, China, 2024120402026@zjou.edu.cn(Y.J.); 2024120402064@zjou.edu.cn(Y.Y.); wbk3122212236@163.com; feidongfly@163.com (F.D.)

2 Shanghai Marine Equipment Research Institute, Shanghai 200031, China, hbljs0221@163.com

3School of Naval Architecture, Ocean and Energy Power Engineering, Wuhan University of Technology, Wuhan430070, China; j.ye@whut.edu.cn (J.Y.)

* Correspondence: yuanqiang@zjou.edu.cn;

Abstract

Ship route planning in complex marine environments is essential for enhancing navigation safety and reducing energy consumption. Conventional algorithms often lack environmental awareness, exhibit limited multi-objective optimization, and are prone to premature convergence. This study proposes an Environment-Aware Adaptive Multi-Objective Ant Colony Optimization (EA-MOACO) algorithm under coupled wind–wave–current conditions.

A marine environmental model using ERA5 reanalysis data and a ship energy-consumption model accounting for current-induced speed correction, wind, and wave resistance are established. An environmental complexity assessment and adaptive parameter adjustment strategy dynamically balance global exploration and local exploitation. A dynamic multi-objective optimization framework integrating route length and energy consumption is implemented using Pareto dominance and ideal-point decision-making.

Experiments show that EA-MOACO outperforms ACO, PSO, MOPSO, NSGA-II, PSO-ACO, and DL-DACO in path length, energy consumption, HV, and IGD. The method provides an efficient, practical framework for intelligent ship route planning in complex marine environments.

Keywords: Ship route planning; Ant colony optimization; Multi - objective optimization; Environmental awareness; Energy consumption model; ERA5; Ocean environment

1. Introduction

With the rapid development of intelligent shipping and autonomous navigation technologies, ship route planning has become an increasingly important research topic in maritime transportation. Efficient route planning not only ensures navigation safety but also significantly reduces voyage distance, fuel consumption, operational costs, and greenhouse gas emissions. Consequently, route optimization plays a vital role in achieving the objectives of intelligent and green shipping. In recent years, with the rapid development of artificial intelligence, big data, and marine observation technologies, autonomous ship navigation systems have gradually emerged as a major research focus in the field of marine engineering. Existing research indicates that ship

route planning is shifting from traditional single-objective optimization toward multi-objective, intelligent, and environment-aware approaches(Yuan, Li et al. 2025) .

Traditional path planning methods primarily include Dijkstra algorithm, the A* algorithm, and dynamic programming methods. These methods typically aim to minimize the shortest path and use graph search strategies to find the optimal path between the start and end points. However, these methods often overlook the impact of marine environmental factors on a vessel's energy consumption during navigation, relying solely on geometric distance as an evaluation metric, which makes it difficult to meet the energy-saving requirements of actual maritime navigation(Chen, Hu et al. 2025). To improve the path planning performance of the A* algorithm, some studies have incorporated environmental factors such as ocean currents, water depth, and traffic regulations into the algorithm(Grifoll, Borén et al. 2022), or enhanced path feasibility by refining the heuristic function(Song, Guo et al. 2024). However, these approaches generally remain focused on single-objective optimization and struggle to accommodate multiple navigation requirements simultaneously.

With the advancement of intelligent technologies, intelligent optimization algorithms such as Genetic Algorithms (GA), Particle Swarm Optimization (PSO), and Ant Colony Optimization (ACO) have been widely applied to ship route planning problems(Liu, Deng et al. 2025). Among these, the Ant Colony Optimization algorithm has demonstrated excellent performance in complex route planning problems due to its strong distributed search capabilities and robustness(Dorigo, Maniezzo et al. 1996). In recent years, researchers have proposed various improvements to the ACO algorithm, such as enhancing obstacle avoidance capabilities by integrating artificial potential field methods(Gao, Zhou et al. 2023) or introducing adaptive mechanisms to optimize search strategies(Liang, Lou et al. 2024). However, traditional ant colony optimization algorithms still face certain limitations in practical applications. For instance, the parameters of the ACO algorithm typically require empirical tuning, and its convergence rate and search capabilities are highly sensitive to parameter combinations(Manazil, Karna et al. 2025). Additionally, traditional ACO lack the ability to dynamically perceive real-time environmental information, making it difficult to adjust search strategies based on environmental complexity(Lazarowska 2015). Furthermore, most studies still focus primarily on single-objective optimization, making it challenging to simultaneously address multiple optimization objectives such as path length and navigation energy consumption.

In response to the aforementioned issues, scholars have in recent years begun to explore the application of multi-objective optimization methods to ship route planning research. For example, multi-objective evolutionary algorithms such as NSGA-II(Deb, Pratap et al. 2002) and MOEA-D(Zhang and Li 2007) can generate a variety of trade-off solutions through Pareto ranking mechanisms; however, these methods often suffer from slow convergence rates in discrete grid environments. On the other hand, some studies have begun to incorporate marine environmental factors into path planning models, using coupled wind-wave-current models to evaluate ship energy consumption; however, how to deeply integrate environmental information with

intelligent optimization algorithms remains a challenging research problem(Liu, Mao et al. 2019, Song, Guo et al. 2024).

Compared to land-based transportation environments, the marine environment is characterized by greater uncertainty and complexity. During navigation, vessels must not only avoid static obstacles such as islands, shoals, and reefs, but also account for the impact of oceanic dynamic factors—including wind fields, wave fields, and ocean currents—on navigation safety and energy consumption(Gkerekos and Lazakis 2020). However, most existing methods still lack coupled modeling of multiple environmental factors and fail to deeply integrate environmental information at the algorithmic level.

To overcome the aforementioned limitations, this paper proposes an Environment-Aware Adaptive Multi-Objective Ant Colony Optimization (EA-MOACO) algorithm for ship route planning in complex ocean environments. This method comprehensively considers real-world ocean environmental factors and vessel energy consumption characteristics, and incorporates an environmental complexity assessment mechanism that enables the algorithm to dynamically adjust key parameters based on environmental difficulty, thereby improving the algorithm's search performance in complex ocean environments. The main contributions of this work are summarized as follows:

(1) A wind–wave–current coupled ocean environment model based on ERA5 reanalysis data is established, together with a ship energy-consumption model that accounts for ocean-current effects, wind resistance, and wave-added resistance.

(2) An environmental-complexity-driven adaptive parameter adjustment mechanism is developed to dynamically regulate pheromone and heuristic factors according to environmental characteristics and optimization progress.

(3) A dynamic multi-objective optimization framework integrating route length and navigation energy consumption is proposed. The framework combines adaptive weighting, Pareto non-dominated sorting, and ideal-point decision-making strategies to improve optimization performance.

(4) Extensive experiments including ablation studies, robustness analyses, environmental-intensity tests, and comparative evaluations are conducted to validate the effectiveness and superiority of the proposed algorithm.

The remainder of this paper is organized as follows. Section 2 introduces the coupled ocean environment model and ship energy-consumption model. Section 3 presents the proposed EA-MOACO algorithm in detail. Section 4 and section 5 describes the experimental setup and discusses the experimental results. Finally, Section 6 concludes the paper and outlines future research directions.

2. Environmental Modelling and Problem Description

The marine environment plays a critical role in ship route planning, as environmental disturbances directly affect navigational safety, route selection, and energy consumption(Zhang 2019). To realistically characterize the influence of environmental factors on vessel navigation, a coupled wind–wave–current environmental model is established and integrated into the route optimization framework. The constructed environmental field is subsequently incorporated into the

ant colony optimization process to evaluate route cost and energy consumption under realistic ocean conditions.

2.1 Grid-Based Environment Representation

Grid-based modelling is one of the most widely adopted approaches in path-planning applications due to its simplicity, computational efficiency, and ease of implementation. In this study, the navigation area is discretized into a two-dimensional grid map, where each cell is assigned a binary state. A value of 1 denotes an obstacle region, whereas a value of 0 represents a navigable area. The grid representation is illustrated in Figure 1.

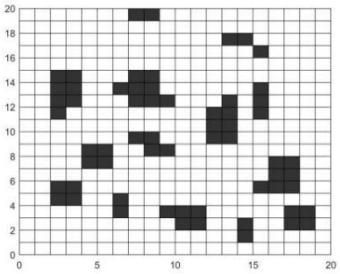


Fig. 1 Schematic diagram of the grid configuration

To ensure accurate localization during route planning, continuous geographical coordinates are transformed into discrete grid coordinates. The vessel position is mapped onto the grid space through a coordinate conversion function, thereby enabling the planning algorithm to efficiently evaluate the spatial relationship between the vessel and surrounding obstacles.

To improve route-search flexibility and navigational realism, an eight-neighbor connectivity structure is adopted. Each grid node can move toward its horizontal, vertical, and diagonal neighboring cells. However, diagonal movements may introduce corner-collision problems when adjacent obstacle cells exist(Li, Dong et al. 2026). Conventional approaches generally address this issue through obstacle expansion, which often reduces feasible navigation space and may even block valid routes.

To overcome this limitation, a collision-constrained transition strategy is employed. As shown in Figure 2, a diagonal transition is permitted only when both adjacent orthogonal cells are navigable. Otherwise, the corresponding diagonal movement is prohibited. This approach effectively eliminates corner-collision risks without enlarging obstacles and establishes a grid transition mechanism that better reflects realistic vessel motion constraints.

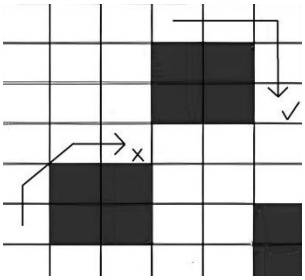


Fig. 2Schematic diagram of the navigation method

2.2 Coupled Wind–Wave–Current Environmental Modelling

Environmental disturbances, including wind, waves, and ocean currents, significantly affect vessel maneuverability, route selection, and energy consumption(Grifoll, Borén et al. 2022). Most existing path-planning studies rely on simplified environmental assumptions, which are insufficient for representing the dynamic characteristics of real marine environments. Therefore, a coupled wind–wave–current environmental field is developed using real meteorological reanalysis data and empirical oceanographic models.

Wind data are obtained directly from the ERA5 reanalysis dataset provided by the European Centre for Medium-Range Weather Forecasts (ECMWF). Wave and ocean-current fields are subsequently constructed using established empirical formulations. The resulting environmental information is mapped onto the route-planning grid and serves as the basis for subsequent energy-consumption estimation and route optimization.

The study area spans 121° E–123° E and 29° N–31° N, corresponding to a one-hour observation period from 08:00 to 09:00 on 8 April 2026. The downloaded ERA5 dataset contains the eastward wind component (u10) and northward wind component (v10) at a height of 10 m above sea level. All environmental data are stored in NetCDF format and processed using MATLAB.

To facilitate integration with the discrete grid environment, bilinear interpolation is employed to project the original latitude–longitude environmental fields onto the route-planning grid.

(1) Wind Field Model

Wind speed and wind direction have a significant impact on a vessel's resistance and course stability. Existing research typically employs spatial functions to simulate wind field distributions(Hou, Tan et al. 2025). This work establishes a two-dimensional wind field model based on ERA5 wind field data. Wind speed and direction are calculated by reading the wind speed components from the dataset. Wind speed is derived from the meridional and zonal wind components, whilst wind direction is calculated using a two-parameter inverse tangent function in accordance with ECMWF ERA5 data processing conventions. The calculation formulas are shown in Equations 1 and 2, respectively, and the wind field models are illustrated in Figures 3 and 4.

$$V_\omega = \sqrt{u_{10}^2 + v_{10}^2} \quad (1)$$

$$\theta_\omega = \arctan\left(\frac{v_{10}}{u_{10}}\right) \quad (2)$$

where V_ω represents wind speed, θ_ω represents wind direction, u_{10} represents the east-west wind component, andv_{10}represents the north-south wind component.

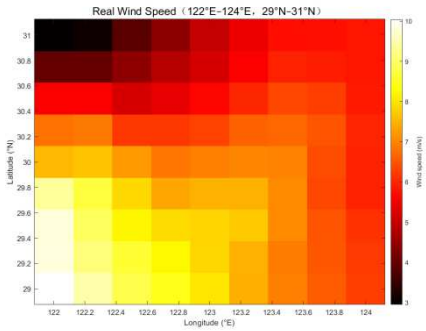


Fig. 3Wind Speed Map

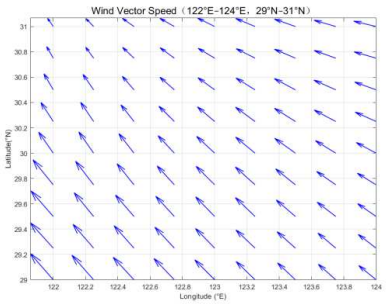


Fig. 4Wind direction map

(2) Wave Model

Wave conditions influence vessel resistance, motion stability, and fuel consumption. Previous studies have demonstrated a strong correlation between wave height and additional ship resistance(Atsuo Maki 2010). In this work, the Significant Wave Height (SWH) is adopted as the primary descriptor of sea-state conditions, the SWH is defined by Equation 3:

$$H_s = \frac{1}{N/3}\sum_{i=1}^{N/3} H_i \qquad (3)$$

where H_s is the significant wave height, and H_i is the height of the top one-third of the wave height series.

Concurrently, this study utilizes the average wave direction D_w as the wave propagation direction to construct the wave direction field. The wave model is illustrated in Figure 5.

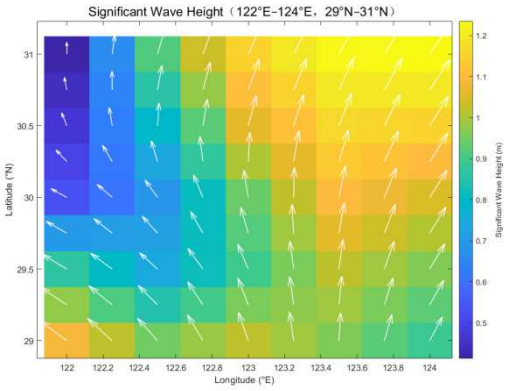


Fig. 5Wave Model

(2) Ocean Current Model

Ocean currents have a direct impact on a vessel's speed and heading. Particularly during coastal navigation, the judicious utilization of favorable currents can significantly reduce energy consumption during navigation(Deb, Pratap et al. 2002). Since the selected ERA5 dataset lacks ocean current variables, and considering that the focus of this study is on the evaluation of route planning algorithms rather than ocean circulation simulation, this study adopted an empirical ocean current model and constructed an ocean current field based on an empirical model of the marine environment. According to the surface wind-drift theory of, surface current velocity is typically approximately 1%–4% of the local wind speed. To balance model simplicity with engineering applicability(Mellor and Mellor 1996), this study selects a wind-drift coefficient of $k_c = 0.02$ and constructs the current field using the wind-induced current approximation model shown in Equations 4 and 5:

$$u_c = k_c u_{10} \tag{4}$$

$$v_c = k_c v_{10} \tag{5}$$

The ocean current velocity and direction are further calculated using Equations 6 and 7:

$$V_c = \sqrt{u_c^2 + v_c^2} \tag{6}$$

$$\theta_c = arctan2(u_c, v_c) \tag{7}$$

where v_c is the ocean current velocity, and θ_c is the ocean current direction.

2.3 Ship Energy Consumption Model

In the route planning process, energy consumption is one of the key indicators for evaluating the quality of a route. Existing research typically establishes energy consumption models based on factors such as speed, resistance and environmental conditions(Guo, Hong et al. 2024, Zhu, Shen et al. 2025). To evaluate route economy under environmental disturbances, a coupled wind–wave–current energy-consumption model is developed.

2.3.1 Speed Model

A vessel's effective speed is influenced by ocean currents. Taking the effect of ocean currents into account, the speed is calculated based on Equation 8:

$$V_{eff} = V_s - V_c * \cos\theta \tag{8}$$

Where V_{eff} is the ship's effective speed, V_s is the ship's own speed, V_c is the current velocity, and θ is the angle between the current direction and the ship's heading. This model accurately reflects the ship's actual speed under the influence of ocean currents.

2.3.2 Resistance Model

In complex marine environments, a vessel's energy consumption during navigation is influenced not only by the distance travelled but is also closely related to environmental disturbances such as wind fields, waves and ocean currents. A vessel's

navigational resistance is primarily composed of frictional resistance and additional environmental resistance. Wind and wave conditions can significantly increase additional resistance(Atsuo Maki 2010).

To enhance the engineering applicability of the route planning results, this paper establishes a wind-wave-current coupled ship energy consumption model and integrates it into the ant colony algorithm route search process. The total ship resistance is divided into three components, as shown in Equation 9: hydrostatic friction resistance, wind resistance, and wave-induced resistance:

$$R = R_f + R_{wind} + R_{wave} \tag{9}$$

In this context, R_f represents hydrostatic drag, R_{wind} represents wind resistance, and R_{wave} represents wave-induced resistance.

(1) Ship Hydrodynamic Resistance

This research employs the ITTC-1957 friction resistance model to calculate the ship's hydrostatic resistance. The ship's Reynolds number is defined as shown in Equation 10:

$$R_e = \frac{V_{eff} L}{v} \tag{10}$$

where L is the ship's length, andv is the hydrodynamic viscosity coefficient.

The friction resistance coefficient is defined as shown in Equation 11:

$$C_f = \frac{0.075}{(log_{10}^{Re} - 2)^2} \tag{11}$$

The ship's frictional resistance is given by Equation 12:

$$R_f = \frac{1}{2} \rho S C_f V_{eff}^2 \tag{12}$$

where ρ is the density of seawater, S is the wet hull surface area, and C_f is the friction drag coefficient.

(2) Wind resistance

Wind fields impose additional aerodynamic drag on a ship. The empirical wind resistance model shown in Equation 13 is used to calculate wind resistance:

$$R_{wind} = \frac{1}{2} \rho_a C_a A_f V_\omega^2 \tag{13}$$

where ρ_a is the density of air, C_a is the air resistance coefficient, A_f is the ship's windward area, and V_ω is the wind speed.

(3) Wave resistance

Waves induce additional motion and resistance in the hull, thereby increasing the vessel's propulsion power requirements. The wave resistance model is shown in Equation 14 to determine the additional wave resistance:

$$R_{wave} = k_\omega {H_s}^2 \tag{14}$$

where H_s is the effective wave height, and k_ω is the empirical coefficient for wave resistance.

2.3.3 Energy Consumption Calculation

A ship's energy consumption is typically positively correlated with resistance

and speed(Deb, Pratap et al. 2002). The energy consumption per unit distance travelled can be calculated using the formula shown in Equation 15:

$$E = R * V_{eff} * t \quad (15)$$

where E is the energy consumption per path segment, R is the total ship resistance, V_{eff} is the effective ship speed, andt is the voyage duration.

3 Environment-Aware Adaptive Multi-Objective Ant Colony Optimization

Traditional ant colony optimization (ACO) algorithms generally employ fixed parameter settings and distance-based heuristic information. Although such approaches perform effectively in static environments, their performance deteriorates in complex marine environments characterized by dynamic wind–wave–current interactions. Fixed parameters may result in premature convergence, while distance-oriented search strategies often neglect the impact of environmental disturbances on navigation cost and energy consumption.

To address these limitations, an Environment-Aware Adaptive Multi-Objective Ant Colony Optimization (EA-MOACO) algorithm is developed. The proposed framework incorporates three key components:

1. environmental complexity assessment;
2. adaptive parameter control;
3. energy-aware multi-objective search.

By integrating environmental information into both the search mechanism and objective evaluation process, the algorithm dynamically balances exploration and exploitation while simultaneously optimizing path length and energy consumption.

The overall framework of EA-MOACO is illustrated in Figure 6.

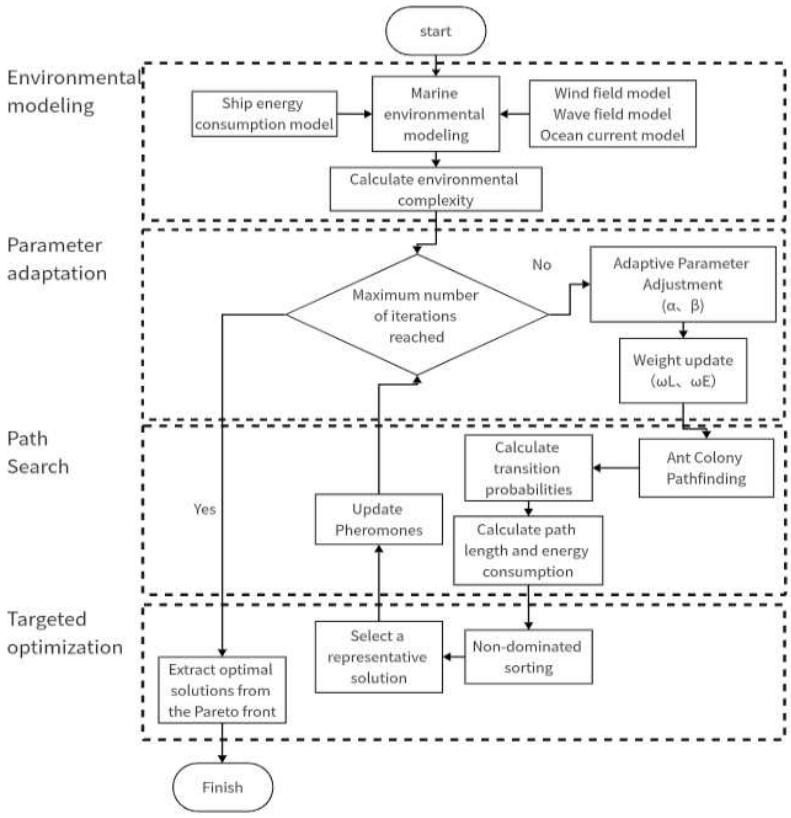


Fig. 6Algorithm Flowchart

3.1 Environmental Complexity Assessment

The search difficulty of ship route planning is highly dependent on environmental characteristics. Existing studies commonly evaluate environmental complexity using obstacle density alone(Liu, Xu et al. 2016). However, obstacle distribution cannot fully characterize the difficulty of long-distance navigation tasks. In traditional path planning algorithms, algorithm parameters are usually fixed and cannot adapt to differences in search difficulty across different environments.

Therefore, a composite environmental complexity index is introduced by considering both obstacle density and task scale. Environmental complexity C is determined jointly by the distribution characteristics of obstacles and the scale of the task space; this metric is defined as shown in Equation 16:

$$C = 0.5\rho_{obs} + 0.5d_{norm} \quad (16)$$

where: ρ_{obs} is the obstacle density factor, representing the proportion of obstacles within the navigable area; $\mathrm{d_{norm}}$ is the normalized value of the distance between the start and end points.

Tab. 1Environmental Complexity Indicators

Environmental Complexity	Environmental Grade
Complexity < 0.5	Simple Environment
$0.5 \leq$Complexity ≤ 0.65	Moderate environment
Complexity > 0.65	Complex environment

Drawing on environment modelling methods commonly used in existing path

planning research, the environment is categorized into three types: simple, moderate and complex(Jun 2009). Obstacle density reflects spatial accessibility, whilst distance reflects task scale; by combining these two factors, the search difficulty can be comprehensively assessed. The comprehensive environment complexity metric is shown in Table 1 and is used to guide subsequent parameter adaptation.

3.2 Parameter Adaptation Mechanism

In traditional ACO, the pheromone importance factor (α) and the heuristic importance factor (β) are typically fixed values. However, research indicates that fixed parameters may result in slow convergence in simple environments and may lead to getting stuck in local optima in complex environments(Chen, Bai et al. 2021, Li, Dong et al. 2026). To improve search adaptability, a two-stage parameter adjustment mechanism is developed. The proposed strategy consists of:

1. environment-driven initialization;
2. iteration-driven dynamic adaptation.

3.2.1 Basic Adjustment Based on Environmental Complexity

Different environmental conditions require different search behaviors.

In simple environments, rapid convergence is desirable and pheromone information should play a dominant role. In contrast, complex environments require stronger exploration capability to avoid premature convergence.

Therefore, the initial values of α and β are selected according to environmental complexity, as summarized in Table 2.

Tab. 2Initial values of parameters for the adaptive adjustment mechanism

Environmental Complexity	α_0(Pheromone weight)	β_0 (Heuristic function weight)	Search Strategy
Simple Environment	1.5	0.8	Faster convergence
Moderate environment	1.0	1.0	Balanced search
Complex environment	0.5	1.5	Enhanced Search

As environmental complexity increases, the pheromone influence is gradually weakened, while the contribution of heuristic information is strengthened.

This mechanism enables the algorithm to adapt its search behavior before the optimization process begins.

3.2.2Iteration-Driven Dynamic Adaptation

To further balance global exploration and local exploitation, the parameter values are dynamically adjusted during optimization.

$$\alpha = \alpha_0 \ （1 + 3 * N/t）\quad （17）$$

$$\beta = \beta_0 \ （1 - 0.5 * N/t）\quad （18）$$

where Ndenotes the current iteration number and trepresents the maximum number of iterations.

Based on Equations 17 and 18, α and β are dynamically adjusted. At the early

search stage, a relatively large β encourages exploration guided by heuristic information. As optimization progresses, α gradually increases while β decreases, enabling the algorithm to exploit high-quality pheromone trails and accelerate convergence(Liu, Wang et al. 2024).

Consequently, the proposed mechanism establishes a dynamic transition from exploration to exploitation.

3.3 Improved Heuristic Function

3.3.1 Definition of the heuristic function

In Traditional ACO defines heuristic information solely according to geometric distance. However, in realistic marine environments, the shortest path does not necessarily correspond to the most economical route.

To incorporate environmental effects into the search process, an energy-aware heuristic function is constructed. Before heuristic calculation, path length and energy consumption are normalized to eliminate dimensional inconsistency. The improved heuristic function as shown in Equation 19:

$$\eta_{ij} = \frac{1}{d_{ij} + \lambda E_{ij}^{norm}} \tag{19}$$

$$\lambda = 0.3 + 0.4C \tag{20}$$

where d_{ij} is the current step distance, E_{ij}^{norm} is the normalised energy consumption value of the path segment. C is the environmental complexity, $C \in [0,1]$. λ represents the energy consumption adjustment weight, $\lambda \in [0.3,0.7]$, with upper and lower bounds set to prevent path length or energy consumption from completely dominating the search. This formulation enables the algorithm to automatically increase the importance of energy consumption in complex environments while maintaining distance-oriented search in simple environments.

3.3.2 The role of the heuristic function in the probabilistic transition formula

The probability of an improved ant moving from nodei to nodej is shown in Equation 21:

$$P_{ij}^{k} = \left[\tau_{ij}\right]^{\alpha}\left[\eta_{ij}\right]^{\beta} \tag{21}$$

where τ_{ij} represents pheromone concentration and η_{ij} represents the heuristic function. In the traditional ant colony algorithm, the probability transition is based solely on geometric distance for path search, whereas the improved probability transition formula is influenced by pheromone concentration, distance and energy consumption

In response to the issue that the traditional ant colony algorithm's heuristic function ignores environmental factors, a multi-objective heuristic function is proposed that integrates path length and energy consumption. By introducing energy consumption normalization and an adjustment parameter driven by environmental complexity, adaptive adjustment of the search strategy is achieved. This method not only improves the physical rationality of path planning but also enhances the

algorithm's robustness and optimization performance in complex marine environments.

3.4 Multi-objective Optimization Strategy

To simultaneously optimize route efficiency and energy economy, a hierarchical multi-objective optimization framework is developed. The proposed framework consists of four components: objective normalization, dynamic weight adjustment, Pareto-based solution evaluation, and ideal-point decision making. By integrating these components, the algorithm can effectively balance the trade-off between path length and energy consumption under varying environmental conditions.

3.4.1 Objective Normalization

Path length and energy consumption differ substantially in both physical units and numerical magnitude. Direct aggregation of these objectives may lead to one objective dominating the optimization process. Therefore, a min–max normalization procedure is applied before fitness evaluation, each objective is normalized using Equations 22 and 23. Let the path length be L and the total energy consumption be E:

$$L_{norm} = \frac{L - L_{min}}{L_{max} - L_{min} + \varepsilon} \quad (22)$$

$$E_{norm} = \frac{E - E_{min}}{E_{max} - E_{min} + \varepsilon} \quad (23)$$

where, L_{max} and L_{min} represent the maximum and minimum path lengths of the current population, E_{max} represents the maximum and minimum energy consumption of the current population, and ε is a very small constant used to prevent the denominator from becoming zero.

Through normalization, both objectives are transformed into dimensionless quantities within a comparable range, thereby improving the stability and fairness of subsequent multi-objective optimization.

3.4.2 Dynamic Weighting Mechanism

In multi-objective path planning, path length L and energy consumption E typically conflict with one another. Traditional methods often employ fixed weights, as shown in Equation 24, to transform the multi-objective problem into a single-objective optimization:

$$F = \omega_L * L + \omega_E * E \quad (24)$$

where ω_L and ω_E are the weight coefficients for path length and energy consumption, respectively.

However, fixed weighting strategies cannot adequately reflect the changing optimization requirements throughout the search process and often exhibit poor adaptability to different environmental conditions(Zhu, Kong et al. 2025). To overcome this limitation, a dynamic weighting mechanism incorporating both iteration progress and environmental complexity is developed.

(1) Base Weights Based on Iteration Progress

The base weights for path length and energy consumption are defined according to the algorithm's iteration progress using Equations 25 and 26 below.

$$\omega_L^{base} = 1 - \frac{iter}{\max_iter} \quad (25)$$

$$\omega_E^{base} = \frac{iter}{\max_iter} \quad (26)$$

Where iter is the current iteration number, and max_iter is the maximum number of iterations.

At the early search stage, the path-length objective receives a larger weight, allowing the algorithm to rapidly identify feasible routes. As the optimization progresses, the importance of energy consumption gradually increases, enabling more refined route optimization.

(2) Environmental Complexity Correction Mechanism

The search stage alone cannot fully capture environmental characteristics. Therefore, environmental complexity (C) is further introduced via Equation 27 and 28 to adjust the objective weights:

$$\omega_E^{env} = min(0.3, 0.3C) \quad (27)$$

$$\omega_L^{env} = -\omega_E^{env} \quad (28)$$

As environmental complexity increases, greater emphasis is placed on energy consumption optimization, while the importance of path length is correspondingly reduced. To prevent excessive bias toward energy-efficient detours, an upper bound is imposed on the environmental correction term.

(3) Weight Fusion and Normalization

The final weights are obtained by combining the base terms and the environmental correction terms, as shown in Equations 29 and 30:

$$\omega_L = \omega_L^{base} + \omega_L^{env} \quad (29)$$

$$\omega_E = \omega_E^{base} - \omega_E^{env} \quad (30)$$

In parallel normalization processing, the final weights are calculated as shown in Equations 31 and 32:

$$\omega_L = \frac{\omega_L^{base} - \omega_E^{env}}{\omega_L^{base} + \omega_E^{base}} \quad (31)$$

$$\omega_E = \frac{\omega_E^{base} + \omega_E^{env}}{\omega_L^{base} + \omega_E^{base}} \quad (32)$$

Additionally, lower bounds of 0.1 are imposed on both weight coefficients to prevent either objective from becoming ineffective during optimization.

The proposed mechanism enables adaptive adjustment in both temporal and spatial dimensions. During early iterations, the algorithm focuses on rapidly identifying short routes, whereas later iterations emphasize energy-efficient refinement. Similarly, in low-complexity environments the optimization favors shorter routes, while in high-complexity environments greater priority is assigned to

energy-efficient navigation. This method enhances energy consumption optimization capabilities whilst ensuring path feasibility, thereby yielding more balanced and engineering-relevant path solutions.

3.4.3 Pareto-Based Solution Evaluation

In complex wind–wave–current coupled marine environments, path length and energy consumption typically present a trade-off. Although dynamic weighting improves optimization flexibility, a single weighted objective cannot fully characterize the trade-off relationship between path length and energy consumption(Dong and Luo 2024). Therefore, Pareto dominance theory is introduced to evaluate candidate solutions. The multi-objective optimization problem can be expressed by Equation 33:

$$minF(x) = \left(L(x),\ E(x)\right) \tag{33}$$

where x represents the sequence of path nodes.

For any two solutions x_1 and x_2, if $L(x_1) \le L(x_2)$, $E(x_1) \le E(x_2)$, and at least one of the inequalities holds strictly, then x_1 is said to dominate x_2. All non-dominated solutions collectively form the Pareto front, which provides a set of alternative routes representing different trade-offs between navigation efficiency and energy consumption. By preserving multiple non-dominated solutions, the algorithm maintains population diversity and avoids premature convergence toward a single objective.

3.4.4 Ideal Point Selection

Building on the above, this paper further introduces an ideal point selection strategy to select the most representative optimal path from the set of Pareto solutions. The ideal point in the normalized objective space is defined as (0, 0), and the Euclidean distance from each Pareto solution to the ideal point is calculated using the formula shown in Equation 34:

$$d = \sqrt{L_{norm}^2 + E_{norm}^2} \tag{34}$$

The solution with the smallest distance is ultimately selected as the output path.

Compared with direct weighted selection methods, the ideal-point approach effectively mitigates the influence of differing objective scales, improves decision consistency, and provides a more balanced compromise between route efficiency and energy consumption.

4 Experimental Setup

To evaluate the effectiveness of the proposed Environment-Aware Adaptive Multi-Objective Ant Colony Optimization (EA-MOACO) algorithm, a series of simulation experiments were conducted under realistic marine environments. The experiments were designed to assess the contributions of individual algorithmic modules, evaluate robustness under stochastic conditions, and investigate adaptability to varying environmental intensities.

All simulations were implemented in MATLAB R2024a and executed on a workstation equipped with an Intel Core i7 processor and 16 GB RAM.

4.1 Experimental Parameter Settings

The main parameters of the proposed algorithm are shown in Table 3.

Tab. 3Main Parameters of the algorithm

Parameter	Meaning	Value
m	Number of ants	50
Nc_max	Maximum number of iterations	100
ρ	Pheromone evaporation coefficient	0.3
Q	Pheromone intensity	1
α	Pheromone factor	Adaptive
β	Heuristic factor	Adaptive

The selection of ship parameters should adequately represent the operational characteristics of typical merchant vessels while maintaining computational efficiency in route-planning simulations. Considering that the objective of this study is to evaluate the effectiveness of the proposed Environment-Aware Adaptive Multi-Objective Ant Colony Optimization (EA-MOACO) algorithm rather than perform full-scale ship performance prediction, a representative medium-sized cargo vessel is adopted as the simulation platform.



Fig. 7 Schematic diagram of the reference cargo vessel

The modeled vessel has a length of 120 m and a wetted surface area of 3000 m², which are consistent with the typical dimensions of medium-sized bulk carriers and multi-purpose cargo ships operating in coastal and offshore waters. The seawater density and kinematic viscosity are set to 1025 kg/m³ and 1.0×10^{-6} m²/s, respectively. To account for environmental disturbances, the aerodynamic drag coefficient is set to 0.8 and the frontal projected area is assumed to be 800 m². In addition, wave-induced added resistance is estimated using an empirical coefficient of 500. The selected vessel parameters are representative of medium-sized merchant vessels commonly operating in East Asian coastal waters. The main parameters of the ship are detailed in Table 4. A schematic diagram of the reference vessel is shown in Figure 7.

Tab. 4 Principal particulars of the reference vessel

Item	Value
Vessel type	Medium-sized cargo ship
Length overall (LOA)	120m

Deadweight (DWT)	10,000t
Service speed	15kn
Wetted surface area	3000m^2
Frontal projected area	800m^2
Air drag coefficient	0.8
Seawater density	1025 kg/m^3
Air density	1.225 kg/m^3
Kinematic viscosity	1.0×10^{-6} m^2/s
Wave resistance coefficient	500

The vessel is assumed to navigate in a wind–wave–current coupled marine environment derived from ERA5 reanalysis data. During route planning, the optimization objective is to simultaneously minimize sailing distance and energy consumption while ensuring safe navigation. All comparative algorithms employ the same vessel model and environmental conditions to guarantee a fair performance evaluation.

4.2 Evaluation Metrics for Multi-objective Algorithms

（1）Hypervolume

Hypervolume (HV) is one of the most widely adopted indicators for evaluating multi-objective optimization algorithms. It measures the volume of the objective space dominated by the obtained Pareto front with respect to a predefined reference point.

A larger HV value indicates that the solution set achieves both better convergence toward the optimal frontier and better diversity across the objective space. Therefore, HV simultaneously reflects solution quality and distribution characteristics.

(3) IGD

The Inverted Generational Distance (IGD) metric evaluates the average distance between the obtained Pareto front and the reference Pareto frontier.

A smaller IGD value indicates that the generated solutions are closer to the true Pareto-optimal set and therefore possess better convergence performance. In ship route planning, a low IGD value implies that the algorithm can effectively identify balanced trade-off solutions between path length and energy consumption.

4.3 Stepwise Ablation Experiments

To verify the effectiveness and necessity of each key module in the proposed environment-aware adaptive multi-objective ant colony algorithm, this study designed a systematic ablation experiment. Each set of experiments was run independently 50 times, with statistics collected on path length, energy consumption, HV, IGD and runtime.

Each set of experiments was run independently 50 times, and path length, energy consumption, multi-objective metrics (HV, Spread, IGD) and running time were recorded to systematically evaluate the contribution of each module to the algorithm’s performance. The modified modules and validation objectives for the experimental design are shown in Table 5.

Tab. 5Modified Modules and Validation Objectives for Ablation Experiments

Experiment Name	Modified Module	Verification Objective
Experiment 1: Basic ACO	Basic Ant Colony Optimization + No environmental modelling + Geometric shortest path	Baseline Algorithm
Experiment 2: Environmental Modelling	Basic Ant Colony + Environmental Modelling + Geometric Shortest Path	Verification of wind, wave and current environment perception
Experiment 3: Parameter Adaptation	Basic Ant Colony + Environmental Modelling + Parameter Adaptation + Geometric Shortest Path	Verification of the adaptive mechanisms in α and β
Experiment 4: Multi-objective planning	Basic Ant Colony + Environment Modelling + Parameter Adaptation + Multi - objective	Validation of the Pareto multi-objective mechanism
Experiment 5: EA-MOACO	Basic Ant Colony Optimization + Environmental Modelling + Parameter Adaptation + Multi - objective + Dynamic Weighting	Validation of the dynamic weighting mechanism

In the complex environment shown in Figure 8, the average values of the evaluation metrics obtained from each group of experiments are shown in Table 5 the mean of representative solutions for each experiment as shown in Figure 9.

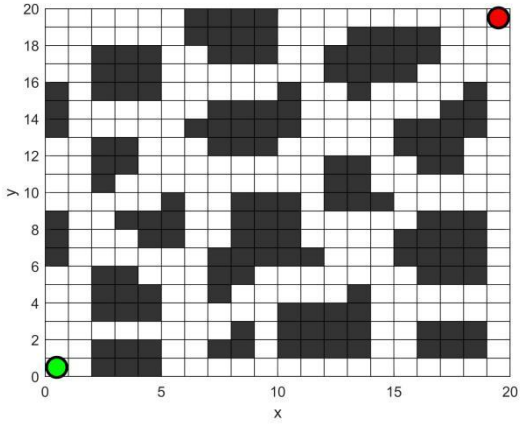


Fig. 8Grid map of ablation experiments

Tab. 6Evaluation metric results for ablation experiments

Experiment	Path Length		Energy Consumption		Runtime		HV		IGD	
	Mean	variance	Mean	Variance	Mean	Variance	Mean	variance	Mean	variance
Experiment 1: Basic ACO	36.104	1.202	9.072×10^6	0.329×10^6	0.427	0.019	0.775	0.093	1.233	0.114
Experi	36.012	1.236	9.031	0.341	0.413	0.020	0.788	0.093	1.217	0.127

ment 2: Environmental Modelling Experiment 3: Adaptive Parameter Experiment 4: Multi-objective Experiment 5 EA-MOACO			$\times 10^6$	$\times 10^6$						
	35.792	1.160	8.989 $\times 10^6$	0.299 $\times 10^6$	0.435	0.018	0.780	0.087	1.211	0.113
	35.632	1.349	8.933 $\times 10^6$	0.362 $\times 10^6$	0.458	0.023	0.812	0.104	1.182	0.172
	35.34	1.073	8.881 $\times 10^6$	0.280 $\times 10^6$	0.448	0.029	0.826	0.082	1.175	0.169

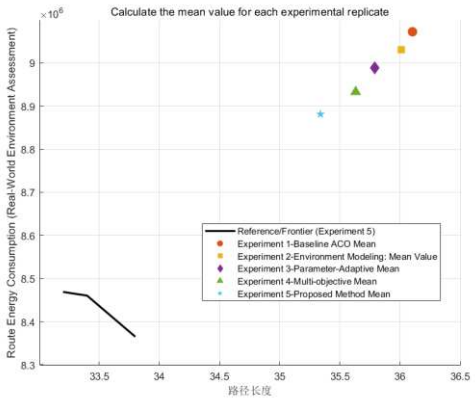


Fig. 9Mean of representative solutions for each experiment

As illustrated in Figure 9, the performance of the algorithm improves progressively as additional modules are incorporated into the optimization framework. This trend demonstrates that each proposed component contributes positively to route-planning performance and validates the effectiveness of the incremental design strategy adopted in EA-MOACO.

Table 6 presents the statistical results for each experimental group. In terms of path length, the environment modelling group showed a 0.25% reduction compared to the baseline ACO, indicating that the algorithm is capable of sensing the distribution of wind, waves and currents to avoid traversing high-cost sea areas, thereby resulting in a slight decrease in path length. The parameter adaptation group showed a 0.86% reduction compared to the baseline ACO, indicating that the parameter adaptation mechanism further enhances search efficiency, leading to a significant reduction in path length. The multi-objective approach achieved a 1.31% reduction compared to

the baseline ACO; the reduction was markedly greater following the introduction of multi-objective optimization, indicating that Pareto search effectively balanced the relationship between path length and energy consumption. Compared with the baseline ACO, the complete EA-MOACO framework reduced the average path length from 36.104 to 35.340, corresponding to an improvement of 2.12%. The improvement can be attributed to the combined effects of environmental awareness and adaptive search mechanisms. By incorporating environmental information into the route evaluation process, the algorithm effectively avoids high-cost regions while maintaining efficient global exploration.

In terms of energy consumption, the environmental modelling approach reduced energy consumption by 0.45% compared to the baseline ACO, indicating that the algorithm is capable of identifying areas of counter-current and high wind and wave conditions, whilst utilizing the advantages of down-current flow. As parameter adaptation improves search efficiency, energy consumption was reduced by 0.91% compared to the baseline ACO; the multi-objective approach reduced energy consumption by 1.53% compared to the baseline ACO, indicating that the multi-objective mechanism has begun to actively consider energy consumption. A more pronounced improvement is observed in energy consumption. The complete EA-MOACO framework reduced average energy consumption from 9.072×10^6 to 8.881×10^6, corresponding to a reduction of 2.11%. Unlike distance-based optimization, the proposed energy-aware objective function explicitly accounts for wind, wave, and current disturbances. Consequently, the algorithm tends to select routes with lower environmental resistance, thereby reducing overall propulsion energy requirements.

In terms of runtime, the environmental modelling enhances the quality of heuristic information compared to the baseline ACO, resulting in a faster search. Although the introduction of the Pareto solution set and non-dominance ordering in Experiment 4 increased computational complexity, leading to a slight rise in runtime, the total computation time remained consistently within 0.04 seconds, indicating that the proposed environment-aware mechanism does not significantly increase the computational burden of the algorithm.

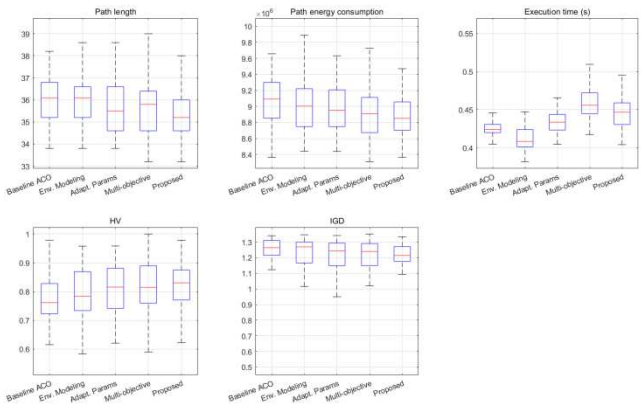


Fig. 10 Box plot of evaluation metrics for ablation experiments

the comparison of average evaluation metrics and box plots of experimental

metrics are shown in Figures 10 and 11.

The environmental information provided by environmental modelling improves the quality of the solution set. The HV of the baseline ACO shows a slight improvement, whilst the multi-objective optimization HV increases by 0.65% compared to the baseline ACO, indicating that the multi-objective mechanism enhances Pareto coverage capability. The HV of EA-MOACO reaches the highest value, improving by 6.58% compared to the baseline experiment, this improvement indicates that the proposed multi-objective framework generates a wider and better-distributed Pareto front. The combination of adaptive weighting and Pareto-based optimization enhances both convergence quality and solution diversity.

Following the incorporation of environmental modelling, the IGD value decreased slightly compared to the baseline experiment, indicating that the search space became more complex and the search difficulty increased. After adding parameter adaptation, the IGD value began to decrease, suggesting that parameter adaptation enhances convergence capability. The IGD value of the complete algorithm decreased by 4.70% compared to the baseline ACO, this result demonstrates that the obtained Pareto solutions are closer to the reference frontier, indicating superior convergence performance. The adaptive parameter adjustment mechanism contributes significantly to this improvement by balancing exploration and exploitation throughout the optimization process.

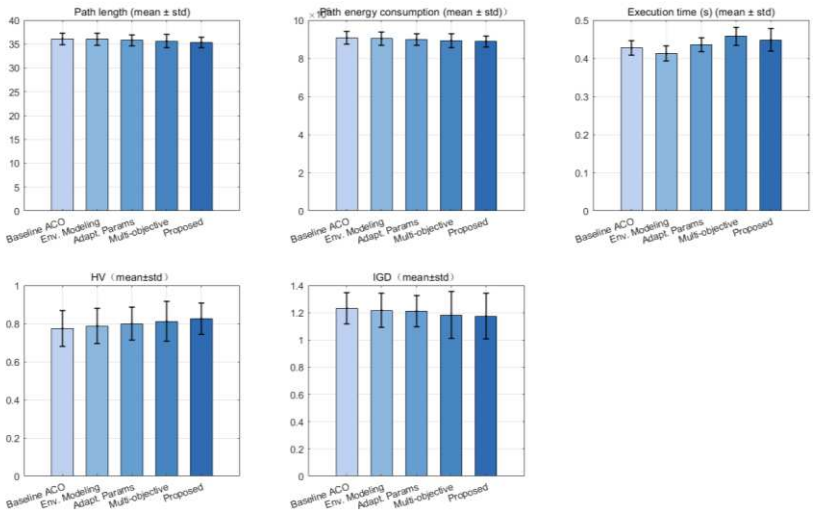


Fig. 11Comparison of mean evaluation metrics

In summary, environmental modelling reduces energy consumption and improves the algorithm's environmental adaptability; the parameter adaptation mechanism enhances convergence accuracy and reduces path length; and multi-objective optimization significantly improves the HV and reduces energy consumption. With the gradual introduction of environmental modelling, the adaptive parameter mechanism and the multi-objective optimization module, the algorithm's overall performance shows a continuous improvement trend. The complete algorithm is capable of achieving shorter paths and lower energy consumption. Consequently, the environment-aware adaptive multi-objective ant colony algorithm proposed in this

paper possesses strong robustness, adaptability and generalization capabilities. It can stably achieve comprehensive optimization of path length, navigation energy consumption and computational efficiency in complex marine environments, thereby providing an effective method for ship path planning in such conditions.

4.4 Robustness Experiments

4.4.1 Independent Repetition Experiments

As the ant colony algorithm is a stochastic intelligent optimization algorithm, its search results are influenced by the initial population distribution, random path selection, and the pheromone update process. To verify the stability and robustness of the proposed EA-MOACO algorithm, 50 independent runs were conducted under identical experimental conditions. A different random seed was used for each run to eliminate the influence of random initialization on the optimization results. Metrics such as optimal path length, optimal path energy consumption, HV, IGD and running time were recorded. The experimental results are shown in Table 7, whilst the scatter plot of path length versus energy consumption and box plots of the various evaluation metrics are shown in Figures 12 and 13, respectively. The convergence curves for HV and IGD are shown in Figure 14.

Tab. 7Results of Independent Repetition Experiments

Metric	Minimum	Maximum	Mean	Standard deviation	Coefficient of Variation (CV)
Optimal path length	33.8	37.4	35.592	0.995	2.80%
Optimal path energy consumption	8.514×10^6	9.458×10^6	8.910×10^6	0.242×10^6	2.72%
Runtime (s)	0.405	0.615	0.478	0.034	7.11%
HV	0.701	0.998	0.871	0.077	8.84%
IGD	0.707	1.354	1.194	0.164	13.74%

As shown in Table 7, EA-MOACO demonstrates good stability across 50 independent runs, with the shortest optimal path length and a standard deviation of only 0.995. The coefficient of variation for optimal path energy consumption is merely 2.72%, indicating that the algorithm is capable of yielding optimization results that are relatively close to one another under different random initialization conditions, and that the search process exhibits good repeatability and reliability. The mean running time of the algorithm in this study is 0.478 s, with a standard deviation of only 0.034 s. This indicates that the computational complexity of the algorithm is relatively stable and does not exhibit significant fluctuations due to the random search process, demonstrating good feasibility for engineering applications. Regarding multi-objective optimization performance, although the standard deviation for HV and IGD fluctuates slightly more than that for path length and energy consumption—as these metrics are more sensitive to the random search process—it remains within a reasonable range. Statistical results show that neither metric exhibits significant instability, indicating that EA-MOACO is capable of consistently obtaining

high-quality Pareto fronts in the majority of runs.

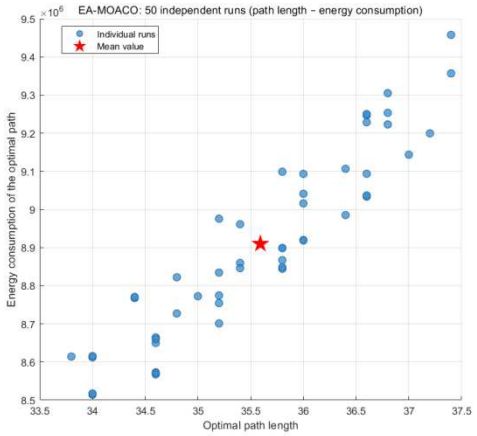


Fig. 12Scatter plot of path length versus energy consumption from independent repeated experiments

Figure 12 presents a three-point distribution plot of optimal path length versus energy consumption obtained from 50 independent replicates. Most samples are concentrated around the mean, with path lengths primarily distributed between 34 and 37, and energy consumption mainly concentrated between $8.6\times10^{6}$to 9.3×10^{6}, indicating that EA-MOACO is capable of consistently obtaining high-quality paths of similar length whilst avoiding local optima, demonstrating good search stability. The scatter plot reveals that all data points cluster around the red mean point, with a strong positive correlation between path length and energy consumption. This phenomenon is consistent with the physical characteristics of vessel navigation, where longer travel distances generally require greater propulsion energy. The concentrated distribution of samples around the mean further confirms the stability of the proposed algorithm.

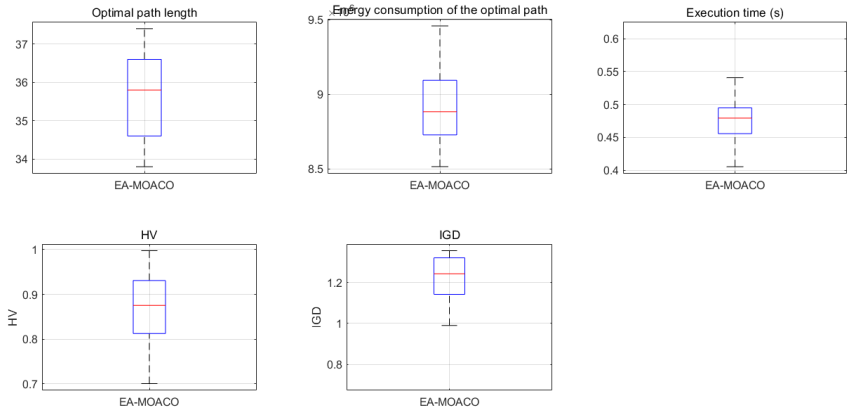


Fig. 13Box-and-whisker plot of evaluation metrics from independent repeated experiments

As shown in the box plot in Figure 13, the boxes for path length and energy consumption are narrow, with the medians close to the center of the boxes, indicating that the data distribution is relatively concentrated and there are no obvious outliers. The range of the runtime box is small, indicating that the algorithm's computational efficiency is stable. The median of the HV metric is close to 0.9, and the interquartile range is small, indicating that EA-MOACO is able to obtain high-quality Pareto

solution sets in most runs, demonstrating good stability in multi-objective optimization. Although the IGD metric exhibits some fluctuation, its overall distribution remains concentrated, with no significant deterioration observed. This indicates that the Pareto solution sets generated by EA-MOACO maintain a small distance from the reference frontier, demonstrating good convergence performance.

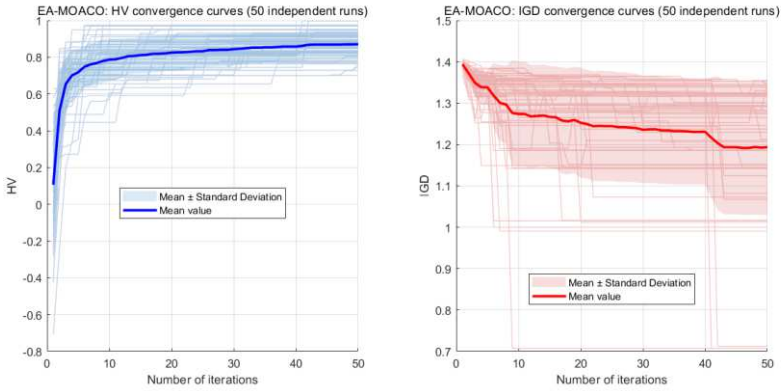


Fig. 14HV/IGD convergence curves

Figure 14 presents the HV and IGD convergence curves from 50 independent runs. The HV convergence curve shows that HV increases rapidly during the initial iteration phase, stabilizes after approximately 20 generations, and ultimately settles above 0.85. This indicates that the algorithm is capable of rapidly constructing a high-quality Pareto frontier and maintaining good solution set coverage. The IGD convergence curve shows that the IGD value continues to decrease throughout the iterative process, eventually stabilizing at around 1.2. This indicates that the Pareto frontier is gradually approaching the true optimal frontier, demonstrating that the algorithm possesses good convergence performance.

In summary, EA-MOACO demonstrated good stability, robustness and convergence across 50 independent runs. The coefficients of variation for path length and energy consumption were both below 3%, whilst the HV and IGD metrics exhibited minimal fluctuation and converged stably. This indicates that the proposed algorithm can effectively mitigate the impact of random factors on optimization results, demonstrating high reliability and engineering application value in complex marine environments.

4.4.2 Experiments under Different Oceanic Environment Intensities

To further validate the environmental adaptability and robustness of the proposed EA-MOACO algorithm in complex marine environments, experiments were designed for different levels of marine environmental intensity. Based on ERA5 real-world marine environmental data, the experiments involved uniformly scaling the ocean current field, wind field and wave field to establish four experimental scenarios: weak environment (kenv=0.5), moderate environment (kenv=1.0), strong environments (kenv=1.5) and extreme environments (kenv=2.0). Each scenario was run independently 50 times, and the mean and standard deviation of each performance metric were calculated to analyze changes in the algorithm's path planning performance under different oceanic disturbance conditions. The mean values of the evaluation metrics are shown in Table 8, the performance variations are illustrated in

Figure 15, the path length–energy consumption distribution is shown in Figure 16, and the trend graphs for the performance metrics are presented in Figure 17.

Tab. 8Experimental results for different oceanic environment intensities

Environmental Intensity	Intensity Coefficient	Path Length		Energy Consumption		Detour Ratio	Energy consumption per unit length
		Mean	Standard deviation	Mean	Standard deviation		
Low	0.5	35.576	1.185	8.426×10^6	2.861×10^5	1.324	2.368×10^5
Medium	1	35.432	1.222	8.876×10^6	3.001×10^5	1.319	2.505×10^5
Strong	1.5	35.604	1.110	9.696×10^6	3.332×10^5	1.325	2.723×10^5
Extreme	2	35.360	1.352	10.640×10^6	4.254×10^5	1.316	3.010×10^5

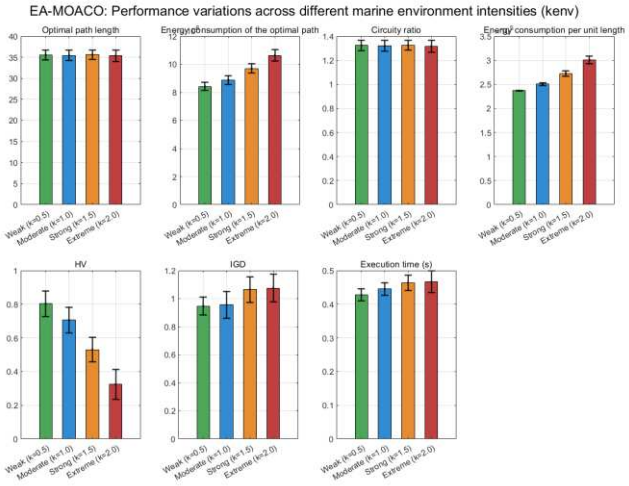


Fig. 15Performance Variations under Different Environmental Intensities

Table 8 and Figure 15 present the statistical results for each environmental intensity. From the overall trend, as environmental intensity gradually increases, path length and detour ratio remain largely stable, whilst energy consumption indicators show an upward trend. The mean path length fluctuated by less than 1%, indicating that changes in environmental intensity have a minimal impact on the length of the planned route. At the same time, the detour ratio also remained within a relatively stable range. The results demonstrate that EA-MOACO is capable of maintaining similar route planning outcomes across different marine environments, without exhibiting significant detours due to increased environmental disturbances, thereby demonstrating good environmental adaptability. As environmental intensity increases, resistance from ocean currents, wind and wave-induced additional resistance all rise simultaneously. Consequently, the vessel requires greater propulsion power to maintain its course; thus, unlike path length, energy consumption exhibits a continuous upward trend as environmental intensity increases. The energy consumption per unit length exhibits a variation pattern consistent with that of total energy consumption, with an increase of 27.11%. This indicates that the rise in energy consumption primarily stems from the increased environmental resistance that must be overcome per unit of voyage distance, rather than additional consumption resulting from an increase in voyage distance. This demonstrates that the wind-wave-current

coupled environmental model constructed in this study can effectively reflect the characteristics of vessel energy consumption variations under different environmental intensities.

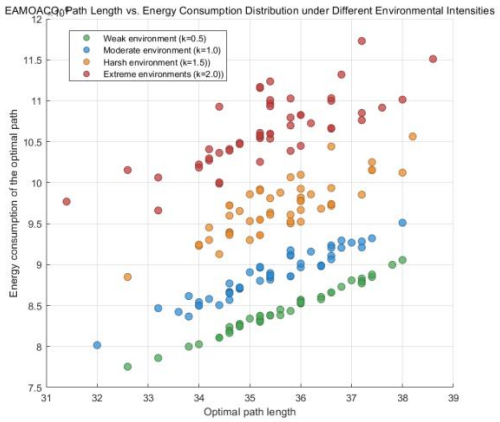


Fig. 16Distribution of path length versus energy consumption under different environmental intensities

Figure 16 presents the distribution of path length versus energy consumption under the same environmental intensity. It can be observed that the four environmental scenarios form a distinct hierarchical structure. As environmental intensity increases, the scatter plot shifts overall towards the high-energy-consumption region, whilst the range of path length distribution remains relatively stable. This indicates that environmental intensity is the primary factor influencing navigation energy consumption, and that EA-MOACO is able to maintain a relatively stable navigation distance through its environmental awareness mechanism.

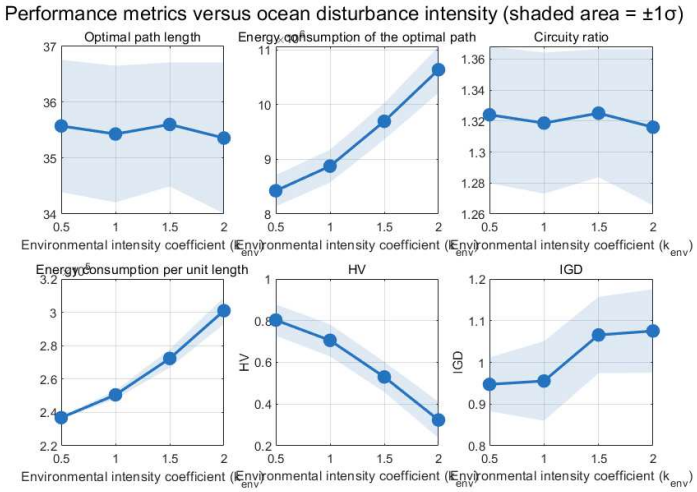


Fig. 17Trend Chart of Performance Metrics

Figure 17 further illustrates the trends of various performance metrics as environmental intensity varies. HV gradually decreases from 0.88 to 0.33, whilst IGD gradually increases from 0.98 to 1.08. This indicates that as the complexity of the marine environment increases, the optimization landscape becomes increasingly challenging due to the amplification of wind, wave, and current-induced disturbances.

Consequently, the Pareto front becomes more difficult to approximate, resulting in a gradual decrease in HV and a corresponding increase in IGD.

Nevertheless, the degradation remains moderate, indicating that EA-MOACO maintains satisfactory optimization capability even under severe environmental disturbances.

In summary, as the intensity of the marine environment increases, the length of the planned route remains stable, whilst changes in energy consumption accurately reflect the growth pattern of environmental resistance. The experimental results validate the effectiveness and robustness of EA-MOACO in complex marine environments, providing reliable support for ship route planning under varying sea conditions.

5. Comparative Experiments

5.1 Experimental Design

To further evaluate the effectiveness and superiority of the proposed Environment-Aware Adaptive Multi-Objective Ant Colony Optimization (EA-MOACO) algorithm, comparative experiments were conducted against several representative path-planning algorithms, including Ant Colony Optimization (ACO), Particle Swarm Optimization (PSO), Multi-Objective Particle Swarm Optimization (MOPSO), Non-Dominated Sorting Genetic Algorithm II (NSGA-II), the Particle Swarm Optimization–Ant Colony Optimization hybrid algorithm (PSO-ACO), and the Deep Learning–Dynamic Ant Colony Optimization algorithm (DL-DACO).

The selected comparison algorithms represent different categories of intelligent optimization methods, including swarm intelligence, evolutionary multi-objective optimization, hybrid optimization strategies, and deep learning-assisted route planning. Consequently, the comparison provides a comprehensive evaluation of the proposed method from the perspectives of route quality, energy efficiency, convergence performance, solution diversity, and robustness.

To ensure a fair comparison, all algorithms were executed under identical environmental conditions, obstacle distributions, and start–goal configurations. The marine environment was constructed using ERA5 reanalysis data, and the wind, wave, and current fields were mapped onto a unified 20×20 planning grid through bilinear interpolation. Each algorithm was independently executed 50 times to reduce the influence of stochastic factors.

5.2 Quantitative Comparison

The representative optimal paths for each algorithm are shown in Figure 18, whilst the mean experimental results are presented in Table 8 and Figure 19.A comparison of the convergence of HV and IGD is shown in Figure 20; the scatter plot of path length versus energy consumption is shown in Figure 21; and the box plots of key performance indicators for each algorithm are shown in Figure 22.

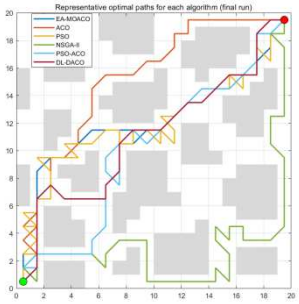


Fig. 18Optimal paths for each algorithm

Tab. 9Side-by-side comparison of mean values

Algorithm Name	HV		IGD		Path Length		Energy consumption		Runtime (s)	
	Mean	Variance	Mean	Variance	Mean	Variance	Mean	Variance	Mean	Variance
EA-MOACO	0.412	0.046	1.372	0.209	35.524	1.170	8.876×10^{6}	3.080×10^{5}	0.528	0.026
ACO	0.390	0.051	1.409	0.018	36.036	1.299	9.037×10^{6}	3.466×10^{5}	0.552	0.025
PSO	-0.073	0.070	1.411	0.012	51.168	2.788	1.271×10^{7}	6.559×10^{5}	0.209	0.007
MOPSO	0.137	0.050	1.408	0.016	43.956	1.701	1.085×10^{7}	3.992×10^{5}	0.270	0.016
NSGA-II	-0.146	0.091	1.411	0.011	54.104	3.828	1.348×10^{7}	9.638×10^{5}	0.223	0.026
PSO-ACO	0.391	0.044	1.396	0.040	36.092	1.164	9.017×10^{6}	3.043×10^{5}	0.395	0.019
DL-DACO	0.406	0.040	1.376	0.084	35.680	1.118	8.916×10^{6}	2.801×10^{5}	0.573	0.027

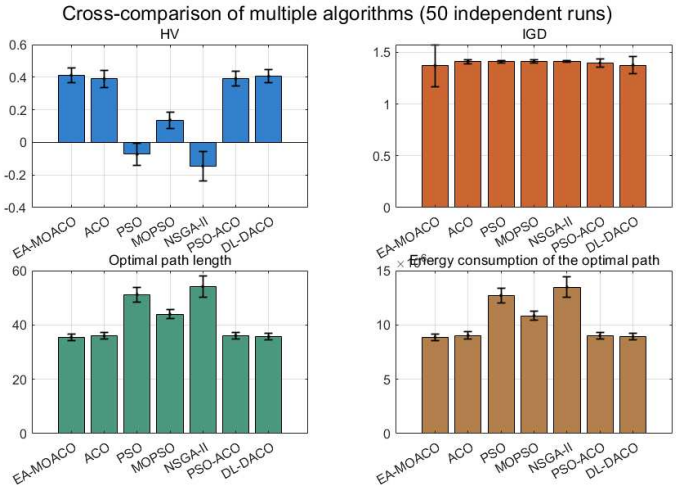


Fig. 19Comparison of algorithm metrics

Table 9 and Figure 19 present the statistical results for each algorithm. The

overall results indicate that EA-MOACO achieved the best performance across key metrics such as HV, IGD, path length and navigation energy consumption.

In terms of multi-objective optimization performance, EA-MOACO achieved the highest HV value, representing an improvement of 5.64% compared to ACO, 5.37% compared to PSO-ACO, and 1.48% compared to DL-DACO. This demonstrates that the environmental awareness mechanism and the multi-objective collaborative optimization strategy effectively enhance the diversity and coverage capability of the solution set.

At the same time, the EA-MOACO algorithm achieved the lowest IGD value, reducing it by 2.63% compared to ACO. The results indicate that EA-MOACO is capable of obtaining a set of non-dominated solutions that is closer to the true Pareto frontier and exhibits a more uniform distribution.

In terms of path quality, EA-MOACO achieved the shortest average path, representing a reduction of 1.47% compared to ACO; regarding energy consumption metrics, EA-MOACO also achieved the lowest average energy consumption, demonstrating that the proposed algorithm can effectively utilize marine environmental information to reduce energy consumption whilst ensuring navigation safety.

EA-MOACO outperforms DL-DACO slightly across all metrics. Given that EA-MOACO does not require deep learning model training or environmental pre-training, it offers superior generalization capabilities and engineering applicability whilst ensuring low energy consumption. Overall, EA-MOACO achieves a good balance between route length and navigation energy consumption, yielding more economical and rational route plans.

5.3 Convergence Analysis

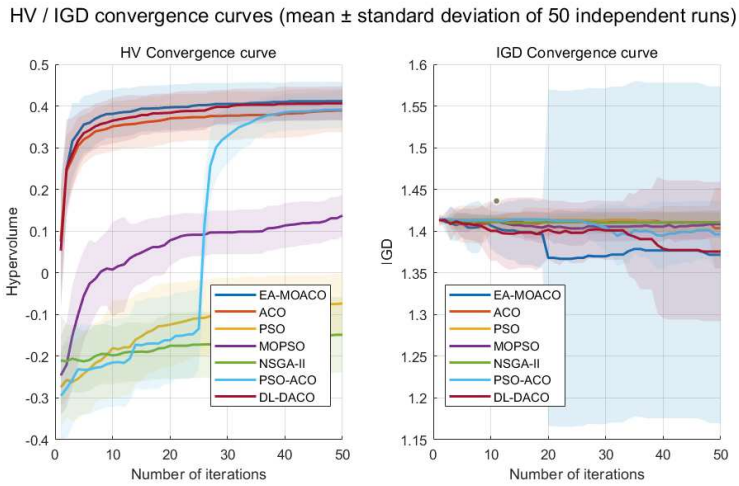


Fig. 20Comparison of HV/IGD Convergence Performance

Figure 20 illustrates the convergence process of HV and IGD.

EA-MOACO demonstrates the fastest increase in HV during the early stages of optimization and reaches a stable high-value region significantly earlier than the comparison algorithms. In contrast, PSO, MOPSO, and NSGA-II exhibit slower convergence and ultimately produce Pareto fronts with substantially lower coverage.

A similar trend can be observed for IGD. Throughout the optimization process,

EA-MOACO consistently maintains lower IGD values and converges more rapidly toward the reference Pareto frontier than ACO, PSO, MOPSO, PSO-ACO, NSGA-II, and DL-DACO.

The superior convergence performance can be attributed to three key factors. First, the environmental-awareness mechanism improves heuristic guidance by incorporating ocean environmental information into route evaluation. Second, the adaptive parameter adjustment strategy dynamically balances exploration and exploitation throughout the search process. Third, the dynamic weighting mechanism improves the coordination between path length and energy consumption objectives, thereby facilitating efficient evolution of the Pareto front. These results demonstrate that EA-MOACO possesses both strong global search capability and excellent convergence efficiency.

5.4 Pareto Front Analysis

Figure 21 compares the Pareto fronts obtained by different algorithms.

The Pareto solutions generated by EA-MOACO are concentrated in the lower-left region of the objective space, indicating superior performance in both path length and energy consumption. Moreover, the obtained solutions are distributed continuously along the frontier without significant gaps, demonstrating strong diversity preservation capability.

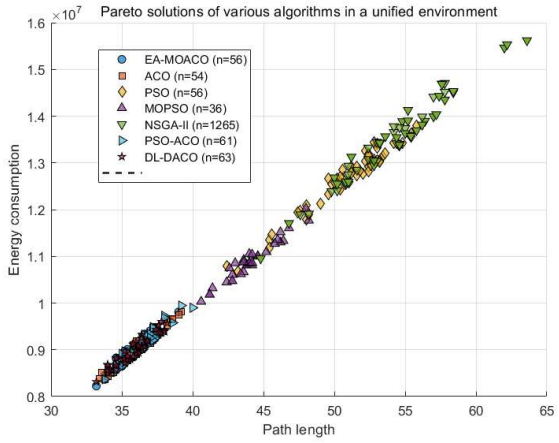


Fig. 21Pareto solutions of various algorithms under a unified environment

Although ACO and PSO-ACO generate several competitive solutions, their Pareto fronts exhibit narrower coverage and lower diversity. This suggests that conventional pheromone-based search strategies remain susceptible to environmental disturbances and are less effective at exploring complex trade-off relationships.

DL-DACO produces a Pareto front that partially overlaps with that of EA-MOACO, indicating that learning-based guidance can improve search quality. However, the frontier generated by DL-DACO remains slightly farther from the reference Pareto front, as reflected by its lower HV and higher IGD values. In contrast, PSO and NSGA-II produce solution sets that are noticeably farther from the reference frontier, indicating weaker convergence capability and poorer adaptability to the coupled wind – wave – current environment. Overall, EA-MOACO achieves the best balance between convergence quality and solution diversity, resulting in a more

representative and practically useful Pareto front for vessel route planning.

5.5 Robustness Comparison

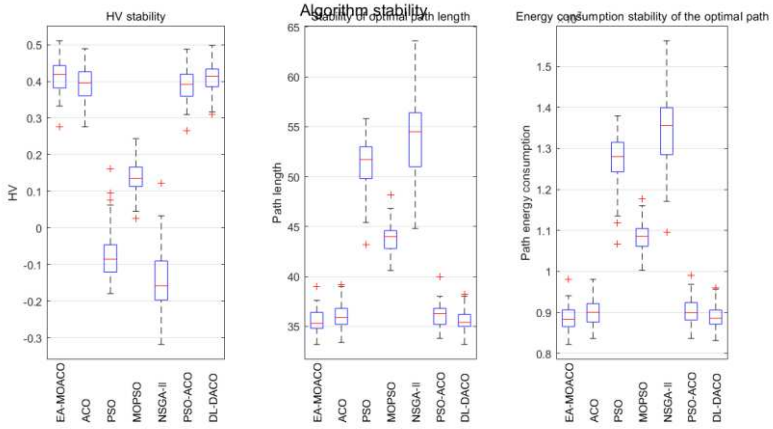


Fig. 22Box-plot of running results

Figure 22 shows a box plot comparing the results of different algorithms.

EA-MOACO exhibits relatively narrow box widths for HV, path length, and energy consumption, indicating limited performance variation across repeated experiments. Furthermore, the median values consistently outperform those of the comparison algorithms.

The reduced dispersion demonstrates that the proposed environmental-awareness and adaptive search mechanisms effectively mitigate the influence of stochastic factors inherent in swarm-intelligence optimization algorithms.

In contrast, PSO and NSGA-II show noticeably larger interquartile ranges and more dispersed distributions, suggesting weaker stability under identical experimental conditions.

The results confirm that EA-MOACO not only achieves superior optimization performance but also maintains strong robustness and repeatability across independent runs.

Based on the above analysis, it can be seen that EA-MOACO fully integrates environmental sensing mechanisms, adaptive parameter tuning, a multi-objective optimization framework, and a dynamic weighting strategy, significantly improving the quality of the Pareto front whilst ensuring a high convergence rate. Compared with traditional ACO, PSO, NSGA-II and the currently advanced DL-DACO algorithms, EA-MOACO achieves shorter paths, lower energy consumption and superior multi-objective optimization performance, validating its effectiveness and superiority in ship route planning within complex marine environments. EA-MOACO achieved the highest HV and lowest IGD among all compared algorithms, indicating that it is not only capable of finding superior non-dominated solutions but also of generating a more uniformly distributed Pareto front, which holds greater practical value for real-world vessel route decision-making.

6. Conclusion

This study proposed an Environment-Aware Adaptive Multi-Objective Ant Colony Optimization (EA-MOACO) algorithm to address the limitations of

conventional ant colony optimization methods in ship route planning under complex marine environments, including insufficient environmental perception, weak multi-objective optimization capability, and susceptibility to premature convergence. By integrating environmental awareness, adaptive parameter adjustment, and multi-objective collaborative optimization into a unified framework, the proposed method enables coordinated optimization of route length and navigation energy consumption under wind – wave – current coupled conditions.

The main conclusions can be summarized as follows:

(1) A wind – wave – current coupled marine environmental model was established based on ERA5 reanalysis data. Wind fields, wave fields, and current fields were mapped onto the route-planning grid through bilinear interpolation, enabling realistic representation of environmental disturbances. Furthermore, a ship energy-consumption model incorporating current-corrected speed, wind resistance, and wave-induced resistance was developed, allowing route evaluation to better reflect actual navigation conditions and improving the practical applicability of the planning framework.

(2) An environmental-complexity-driven adaptive parameter adjustment mechanism was developed. By combining obstacle density and mission-scale information, an environmental complexity index was constructed to characterize the difficulty of the search space. The pheromone factor and heuristic factor were dynamically adjusted according to both environmental complexity and iteration progress, enabling the algorithm to maintain strong exploration capability during the early search stage while enhancing exploitation efficiency in later iterations. This mechanism effectively improves convergence performance and reduces the risk of local optima.

(3) A multi-objective optimization framework integrating route length and navigation energy consumption was designed. Through objective normalization, dynamic weighting, Pareto dominance optimization, and ideal-point decision-making, the proposed framework achieves adaptive coordination between navigation efficiency and energy economy. The resulting Pareto solutions exhibit improved diversity and convergence quality, providing decision-makers with a broader range of feasible route alternatives.

Overall, the proposed EA-MOACO algorithm achieves an effective balance among route length, navigation energy consumption, and computational efficiency. By incorporating realistic environmental information into the optimization process and introducing adaptive multi-objective search mechanisms, the method provides a practical and efficient solution for intelligent ship route planning in dynamic marine environments.

Future research will focus on extending the proposed framework in three directions. First, dynamic environmental updates derived from real-time meteorological and oceanographic observations will be incorporated to support online route replanning. Second, dynamic obstacles, vessel traffic interactions, and maritime traffic regulations will be integrated into the optimization framework to enhance operational realism. Third, advanced intelligent decision-making approaches, such as

deep reinforcement learning, digital twin technology, and multi-agent collaborative optimization, will be explored to further improve autonomous navigation capability and real-time decision-making performance in highly dynamic maritime environments(Chen, Hu et al. 2025, Liu, Deng et al. 2025).

Funding: This research was funded by National Natural Science Foundation of China Key Project: NO. 51839005; High-tech Ship Research Special Project: NO. K24532-1-2; Zhoushan Science and Technology Bureau Fund Project: NO. 2023C41022; National Natural Science Foundation of China: NO. 52101388.

Data Availability Statement： The data supporting the findings of this study are available from publicly accessible sources. The ERA5 reanalysis datasets used in this research can be obtained from the Copernicus Climate Data Store (CDS) (https://cds.climate.copernicus.eu/). The simulation data and MATLAB codes generated during the current study are available from the corresponding author upon reasonable request.

Conflicts of Interest: The authors declare no conflicts of interest.

References

Atsuo Maki, Y. A., Yuichi Nagata (2010). "A Weather Routing System Considering Ship Stability." Proceedings of the Japan Society of Naval and Ocean Engineering Conference: 369–372.

Chen, X., et al. (2025). "Intelligent ship route planning via an A∗ search model enhanced double-deep Q-network." Ocean Engineering 327: 120956.

Chen, Y., et al. (2021). "Path planning and obstacle avoiding of the USV based on improved ACO-APF hybrid algorithm with adaptive early-warning." Ieee Access 9: 40728–40742.

Deb, K., et al. (2002). "A fast and elitist multiobjective genetic algorithm: NSGA-II." IEEE transactions on evolutionary computation 6(2): 182–197.

Dong, Z.-r. and W.-w. Luo (2024). "Ship pipe route design based on NSGA-III and multi-population parallel evolution." Ocean Engineering 293: 116666.

Dorigo, M., et al. (1996). "Ant system: optimization by a colony of cooperating agents." IEEE transactions on systems, man, and cybernetics, part b (cybernetics) 26(1): 29–41.

Gao, P., et al. (2023). "Research on ship collision avoidance path planning based on modified potential field ant colony algorithm." Ocean & Coastal Management 235: 106482.

Gkerekos, C. and I. Lazakis (2020). "A novel, data-driven heuristic framework for vessel weather routing." Ocean Engineering 197: 106887.

Grifoll, M., et al. (2022). "A comprehensive ship weather routing system using CMEMS products and A* algorithm." Ocean Engineering 255: 111427.

Guo, Z., et al. (2024). "Research on safety evaluation and weather routing optimization of ship based on roll dynamics and improved A* algorithm." International Journal of Naval Architecture and Ocean Engineering 16: 100605.

Hou, J., et al. (2025). "Inshore sailing route optimization integrating terrain-influenced wind field." Ocean Engineering 326: 120848.

Jun, G. U. (2009). "Research on a Path Planning Algorithm for Unmanned Intelligent Obstacle Crossing Vehicle." Journal of Chongqing Institute of Technology(Natural Science).

Lazarowska, A. (2015). "Ship's trajectory planning for collision avoidance at sea based on ant colony optimisation." The Journal of Navigation 68(2): 291–307.

Li, J., et al. (2026). "Brachistochrone-Principle-Based Adaptive Ant-Colony Algorithm for Ship Path Planning in Practical Environments." Transportation Research Record 2680(1): 764–780.

Liang, W., et al. (2024). "An enhanced ant colony optimization algorithm for global path planning of deep-sea mining vehicles." Ocean Engineering 301: 117415.

Liu, C., et al. (2019). "An improved A-star algorithm considering water current, traffic separation and berthing for vessel path planning." Applied Sciences 9(6): 1057.

Liu, M., et al. (2016). "Cooperative path planning for multi-AUV in time-varying ocean flows." Journal of Systems Engineering and Electronics 27(3): 612–618.

Liu, Y., et al. (2024). "A quick pheromone matrix adaptation ant colony optimization for dynamic customers in the vehicle routing problem." Journal of Marine Science and Engineering 12(7): 1167.

Liu, Z., et al. (2025). "Ship path planning methods: A state-of-the-art survey." Ocean Engineering 341: 122599.

Manazil, R., et al. (2025). Performance Comparison of PSO, ABC, and ACO Algorithms For Multi-UAV 3D Path Planning and Collision Avoidance. 2025 10th International Conference on Information Technology and Digital Application (ICITDA), IEEE.

Mellor, G. L. and G. Mellor (1996). Introduction to physical oceanography, Springer.

Song, C., et al. (2024). "Ship path planning based on improved multi-scale a* algorithm of collision risk function." Scientific Reports 14(1): 30418.

Yuan, P., et al. (2025). "Optimal path planning and navigation platform development for unmanned surface vehicles in complex inland waterways using a potential ant-colony algorithm." Ocean Engineering 334.

Zhang, M. (2019). "Multi-objective trajectory optimisaton on environmental impacts."

Zhang, Q. and H. Li (2007). "MOEA/D: A multiobjective evolutionary algorithm based on decomposition." IEEE transactions on evolutionary computation 11(6): 712–731.

Zhu, J., et al. (2025). "Energy-efficient route planning method for ships based on level set." Sensors 25(2): 381.

Zhu, M., et al. (2025). "A multi-objective path planning method for ships based on constrained policy optimization." Ocean Engineering 319: 120165.